Selenium nanoparticles: effect of autoclave treatment on size, shape, phase and antimicrobial properties

T. Hesabizadeh [a], R. Subedi [a], T. J. Webster [b,c,d], G. Guisbiers [a,*]
[a] *Department of Physics & Astronomy, University of Arkansas at Little Rock, 2801 South University Avenue, 72204 Little Rock, USA*
[b] *School of Health Sciences & Biomedical Engineering, Hebei University of Technology, China*
[c] *School of Engineering, Saveetha University, Chennai, India*
[d] *Division of Pre-college & Undergraduate Students, Brown University, Providence, USA*

Amorphous selenium nanoparticles have been synthesized by pulsed laser ablation in liquids. After undergoing a thermal treatment at 121°C for 60 minutes, the amorphous nanoparticles crystallized into trigonal ones. The antimicrobial properties of both amorphous and trigonal nanoparticles have been compared; and the amorphous ones displayed better antibacterial and antifungal properties compared to the trigonal ones. Specifically, Methicillin-resistant *Staphylococcus aureus* (MRSA), Ampicillin-resistant *Escherichia coli*, *Pseudomonas aeruginosa*, *Staphylococcus epidermidis*, and *Candida albicans* were almost completely inhibited in the presence of amorphous selenium nanoparticles at 0.025 microgram/ml concentrations after 24 hours of in vitro culture, compared to controls (no nanoparticles). In summary, such a high sensitivity of these bacterial and fungal strains to low concentrations of amorphous selenium nanoparticles warrants further investigation to develop efficient anti-bacterial and anti-fungal treatments.

(Received August 13, 2024; Accepted November 2, 2024)

Keywords: Selenium, Chalcogenides, Antibacterial, Antifungal, Nanoparticles

1. Introduction

Selenium (Se) is a chalcogen element displaying antibacterial [1-6], antifungal [7-12], antiviral [13-15] and anticancer [1, 16-21] properties, since selenium is an antioxidant (i.e., it inhibits oxidation) [22]. Indeed, oxidative stress is an important contributor to the pathophysiology of a variety of conditions such as carcinogenesis and inflammation, generally occurring during a bacterial, fungal or viral infection. Moreover, epidemiological studies demonstrated a reciprocal relationship between selenium intake and cancer mortality [23] as well as inflammation [24]. Consequently, developing Se nanoparticles (NPs) became a hot topic within the scientific community due to its antimicrobial properties in suspended and deposited forms [25-27]. To produce antimicrobial Se NPs, various methods exist such as chemical, biological and physical methods [26, 28]. In this letter, a physical method known as pulsed laser ablation in liquids (PLAL) was chosen to preserve the cleanliness of the surface of the Se NPs being produced [29-32].

2. Experimental

2.1. Synthesis

2.1.1. First step synthesis protocol

Selenium pellets (@99.999% from Sigma-Aldrich) were immersed inside a 50 ml single-neck glass flask containing 5 ml of deionized water. The 5-minutes irradiation was performed at 12.5 W from underneath the container by using a Nd:YAG laser, emitting at 1064 nm and pulsing at 3

* Corresponding author: gxguisbiers@ualr.edu
https://doi.org/10.15251/CL.2024.2111.847

kHz. The laser beam was focused on the Se pellets by using a bi-convex lens (focal length = 16 mm) making an average laser spot size of around ~110±28 μm on the pellets, which corresponds to a laser fluence of ~131±33 Jcm^{-2}.

2.1.2. Second step synthesis protocol

After the first set of irradiations, the target was removed and the colloid was poured into a test tube for another 5-minutes irradiation. This time, the irradiation was performed from the top. The same repetition rate (3 kHz) was used. The test tube was surrounded with ice to avoid excess heating of the solvent. At the end of this second step, the Se NPs were amorphous.

2.1.3. Third step synthesis protocol

A heating treatment using an autoclave at 121°C for 60 minutes was performed to transform the amorphous Se NPs into trigonal Se NPs.

2.2. Characterization

The Zeta potential of colloids was determined by using the NanoBrook 90Plus Zeta from Brookhaven Instruments. Scanning electron microscopy (SEM) imaging was performed using a JEOL-JSM-7000F operating at 15 kV. Finally, Raman spectroscopy was performed using the EZ-N-532-B1S Raman-N from Enwave Optronics, Inc. (532 nm, 50 mW).

2.3. Bacteria assays

For bacteria experiments, Methicillin-resistant *Staphylococcus aureus* (MRSA), Ampicillin-resistant *Escherichia coli*, *Pseudomonas aeruginosa*, *Staphylococcus epidermidis*, and *Candida albicans* (all obtained from ATCC) were separately seeded in Dulbecco's Modified Eagle Medium (DMEM) with 10% Fetal Bovine Serum (FBS from Gibco) at 10^6 CFU/cm^2 into standard 12 well plates (Sigma-Aldrich). The aforementioned Se NPs were then separately added at a concentration of 25±5 ppm (or 0.025 micrograms/ml) and bacteria were cultured for 24 hours. At that time, the media was removed and bacteria numbers determined using standard colony forming units with the spreading and plating method [33-35]. Experiments were repeated three times.

3. Results and discussion

Under normal conditions of temperature and pressure, selenium exists under two forms: amorphous [28, 36] and trigonal [28, 37]. In this letter, amorphous Se NPs were obtained after a two-step synthesis protocol while trigonal Se NPs were obtained after a three-step synthesis protocol (Figure 1a). The first step involves a bottom-ablation [38] synthesis protocol while the second step requires a top-ablation [38] synthesis protocol. The third step is a heating treatment using an autoclave. The colloid obtained after the first two-steps synthesis protocol is shown on Figure 1b (left) while the colloid obtained after the three-step synthesis protocol is shown on Figure 1b (right). The orange color of the colloid (left) is characteristic of amorphous selenium while the grey color of the colloid (right) is characteristic of trigonal selenium. By shining the pointer laser beam through both colloids, the laser beam is being scattered within each colloid indicating the presence of the NPs ("*Tyndall effect*") [39]. The phase of the NPs was confirmed by Raman spectroscopy. Indeed, the orange colloid displayed a Raman peak around 250 cm^{-1} which is characteristic of the Se-Se stretching vibrational mode A_1 of the amorphous phase of selenium (Figure 1c). The same stretching mode A_1 is being displayed around 230 cm^{-1} for the grey colloid, which characteristic of the trigonal phase of selenium (Figure 1d) [40, 41].

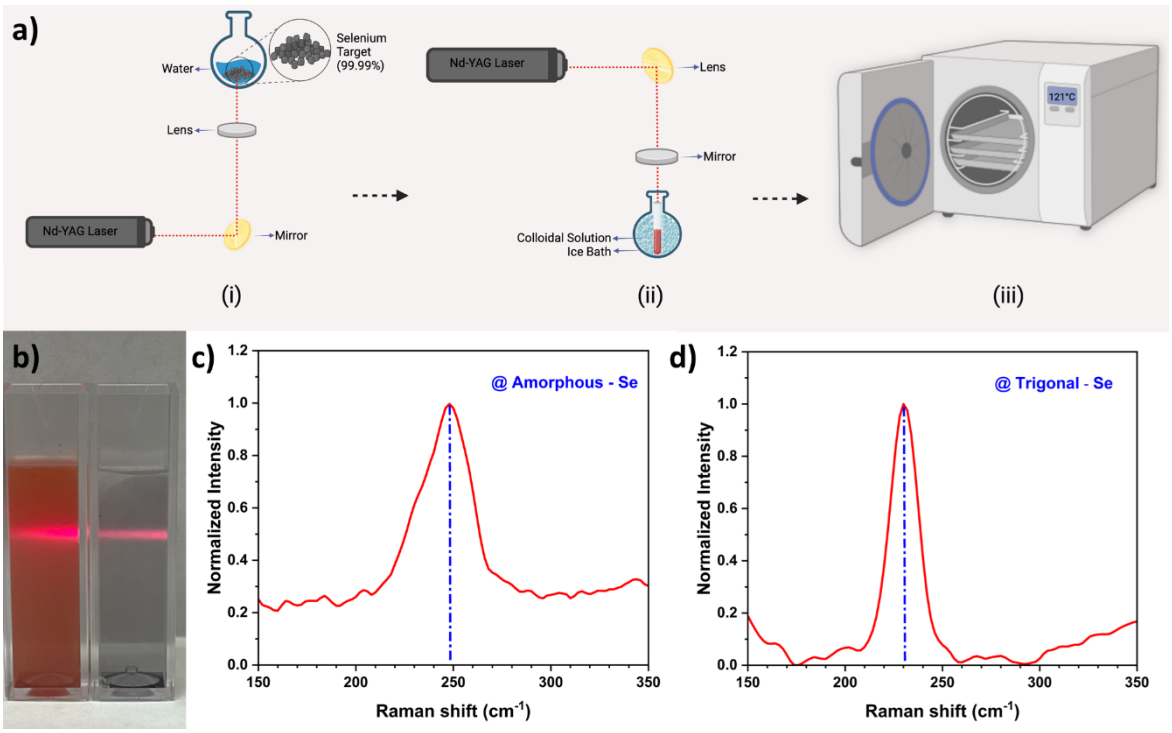

Fig. 1. a) Sketch displaying each step of the synthesis protocol: 1st set of irradiations using a bottom-ablation PLAL set-up (i), 2nd set of irradiations using a top-ablation PLAL set-up (ii), autoclave treatment to induce phase transition (iii). b) Tyndall effect being visible in both colloids containing the amorphous (left) and trigonal (right) Se NPs. c) and d) Raman spectra of amorphous Se NPs and trigonal Se NPs, respectively.

Additionally, SEM was performed on both samples after dropping a small droplet of colloid onto a silicon wafer and letting it dry in air. The amorphous Se NPs were spherical while the trigonal Se NPs were polyhedral (Figure 2a and 2b). On Figure 2b, some needles can even be observed in the upper part of the image. This can be explained by the hexagonal lattice structure of selenium being hexagonal and consequently privileging an anisotropic growth along the c-axis. [42] The size distribution of Se NPs has been measured by using ImageJ software and the average size of amorphous and trigonal Se NPs were determined around 72±29 nm and 320±28 nm, respectively (Figure 2c and 2d).

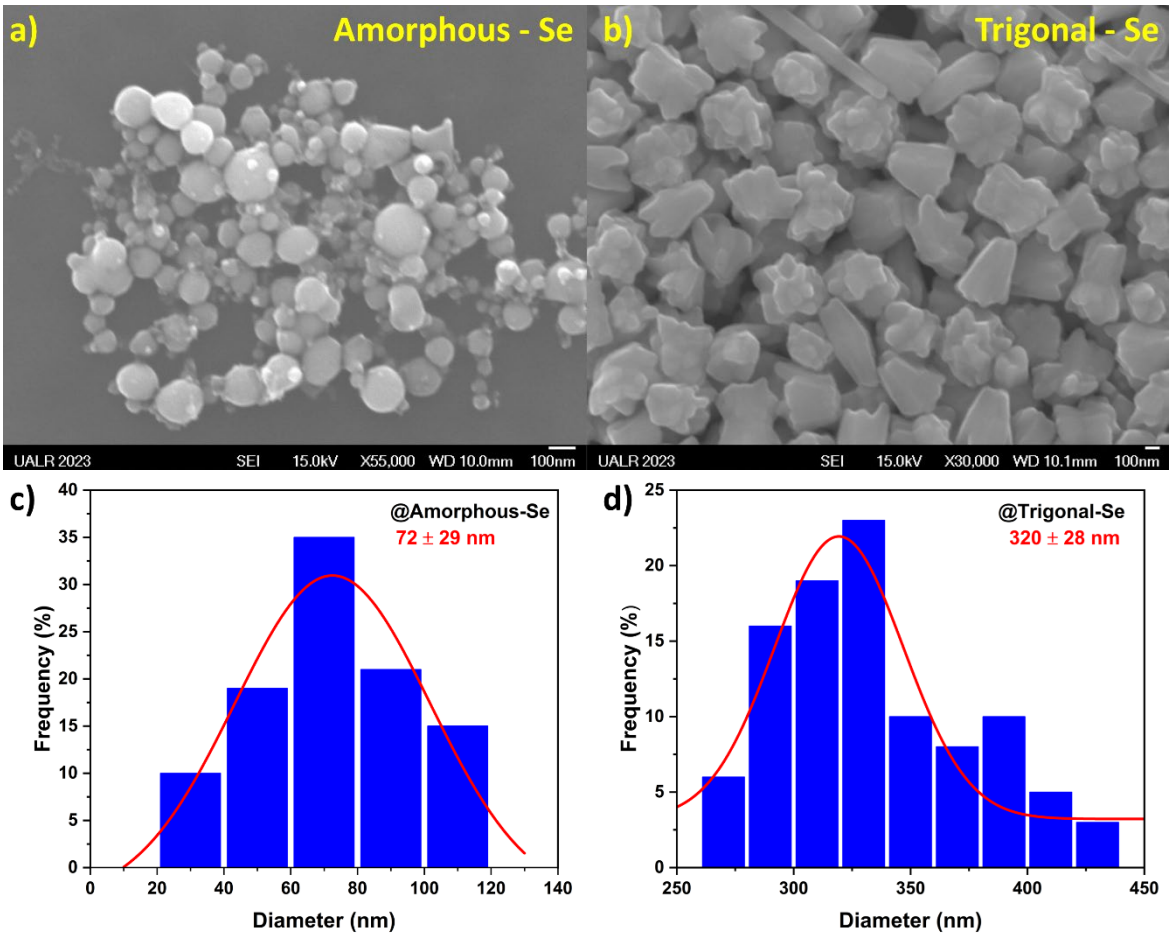

Fig. 2. SEM images of a) amorphous Se NPs and b) trigonal Se NPs. Size distributions of the c) amorphous Se NPs and d) trigonal Se NPs.

The stability of the colloid over time was determined by measuring the Zeta potential. The Zeta potential of amorphous Se NPs was measured at -43±1 mV while the Zeta potential of trigonal Se NPs was around -19±11 mV (Figure 3). By displaying such Zeta potential values, the colloid containing the amorphous Se NPs was considered stable with time while the one containing the trigonal Se NPs was considered unstable. By definition, a colloid displaying a Zeta potential value between -30 mV and +30 mV is considered unstable [43].

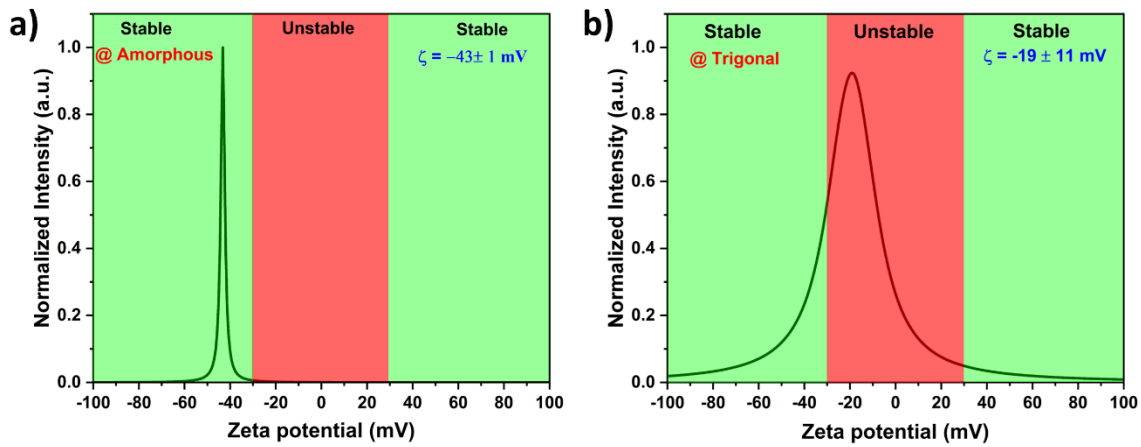

Fig. 3. Zeta potential of the colloids containing a) amorphous Se NPs and b) trigonal Se NPs.

Both types of Se NPs (amorphous and trigonal) stopped the growth of bacteria (Methicillin-resistant *Staphylococcus aureus* (MRSA), Ampicillin-resistant *Escherichia coli*, *Pseudomonas aeruginosa*, *Staphylococcus epidermidis*) and fungus (*Candida albicans*). However, at a given concentration, amorphous Se NPs displayed better antimicrobial properties compared to the trigonal ones (Figure 4). This may be due to the size of amorphous Se NPs being much smaller compared to the trigonal ones and consequently exhibiting a larger surface-to-volume ratio. A second possibility may be the surface energy of amorphous selenium being larger than the surface energy of trigonal selenium.[44, 45] As, the surface energy of bacteria is typically smaller than the surface energy of liquids in which they are suspended, this mismatch causes bacteria to attach preferentially to materials with larger surface energies such as amorphous Se NPs [46, 47]. A third possibility might be a larger electrostatic interaction between the bacteria and the Se NPs. However, most bacteria have a net negative surface charge [46] and interact preferentially with positively charged surfaces which is not the case of neither the amorphous nor the trigonal Se NPs.

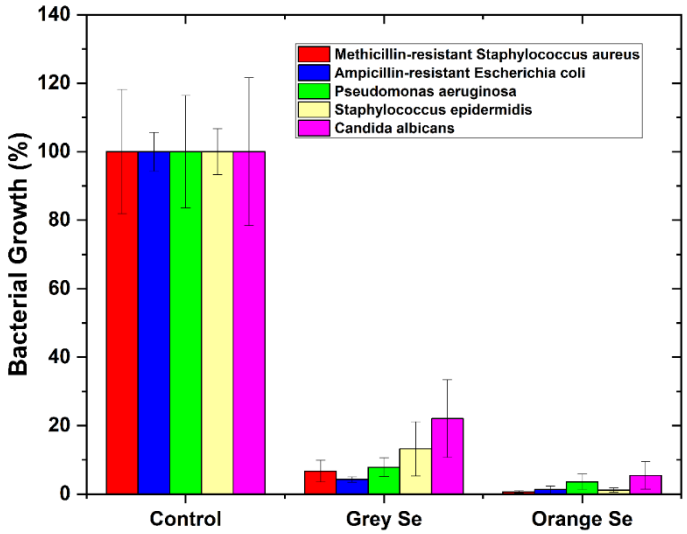

Fig. 4. Colony counting assay of Methicillin-resistant Staphylococcus aureus (MRSA), Ampicillin-resistant Escherichia coli, Pseudomonas aeruginosa, Staphylococcus epidermidis and Candida albicans at 0.025 microgram/ml for 24h in the presence of amorphous (orange) or trigonal (grey) Se NPs. Data = mean; N = 3 (repeated 3 times). All values are statistically different ($p<0.01$) when comparing the same bacteria between controls, grey Se (trigonal), and orange Se (amorphous).

From the literature, it seems that amorphous Se NPs were already preferred in the treatment of some cancers [48]. Moreover, it has been proved recently by Li *et al.*[49] that organisms can transform the amorphous Se NPs into seleno-amino acids but not the trigonal ones suggesting a better assimilation of the amorphous phase of Se by biological organisms. Lastly, studies on amorphous Se NPs have indicated decreased thiol-containing proteins in bacteria and greater generation of reactive oxygen species (ROS), thus, providing a mechanism by which they kill various bacteria, although future studies will be needed to determine how these anti-bacterial and anti-fungal mechanisms compare to trigonal Se NPs [33-35].

4. Conclusions

To conclude, an autoclave treatment increases the size of NPs and may change the phase of the NPs, depending the nature of the chemical element constituting it. Biologically, both forms of selenium NPs were antimicrobial but amorphous Se NPs were more efficient as an antibacterial and antifungal agent as compared to trigonal Se NPs. It seems that it is a combination of factors that

explain why the amorphous Se NPs were exhibiting better antimicrobial properties. The smaller size and higher surface energy of the amorphous phase seems to be the reasons underneath the better performance of amorphous Se NPs compared to the trigonal ones.

Acknowledgments

This publication was made possible by the Arkansas INBRE program, supported by a grant from the National Institute of General Medical Sciences, (NIGMS), P20 GM103429 from the National Institutes of Health (NIH). T. H., R. S. and G.G. would like to thank the Center for Integrative Nanotechnology Sciences (CINS) of UA Little Rock for the use of their SEM.

References

[1]. L.D. Geoffrion, et al., ACS Omega, 5(6), 2660-2669, (2020); https://doi.org/10.1021/acsomega.9b03172

[2]. G. Guisbiers, et al., International Journal of Nanomedicine, 11, 3731-3736, (2016); https://doi.org/10.2147/IJN.S106289

[3]. G. Guisbiers, et al., Laser Physics Letters, 12(1), 016003, (2015); https://doi.org/10.1088/1612-2011/12/1/016003

[4]. B. Ao, et al., Frontiers in Microbiology, 14, 1229838, (2023). https://doi.org/10.3389/fmicb.2023.1229838

[5]. Q.Y. Yuan, et al., Microorganisms, 11(6), 1519, (2023); https://doi.org/10.3390/microorganisms11061519

[6]. T. Huang, et al., Nanoscale, 11(31), 14937-14951, (2019); https://doi.org/10.1039/C9NR04424H

[7]. G. Guisbiers, et al., Nanomedicine-Nanotechnology Biology and Medicine, 13(3), 1095-1103, (2017); https://doi.org/10.1016/j.nano.2016.10.011

[8]. H.H. Lara, et al., International Journal of Nanomedicine, 13, 2697-2708, (2018); https://doi.org/10.2147/IJN.S151285

[9]. Z. Toprakcioglu, et al., ACS Applied Materials & Interfaces, 15, 10452-10463, (2023); https://doi.org/10.1021/acsami.2c21013

[10]. D.A. Serov, et al., Materials, 16(15), 5363, (2023); https://doi.org/10.3390/ma16155363

[11]. M. Shakibaie, N.S. Mohazab, and S.A.A. Mousavi, Jundishapur Journal of Microbiology, 8(9), e26381, (2015); https://doi.org/10.5812/jjm.26381

[12]. H.G. Lazcano-Ramírez, et al., Antibiotics-Basel, 12(1), 115, (2023); https://doi.org/10.3390/antibiotics12010115

[13]. A. Khurana, et al., Journal of Drug Delivery Science and Technology, 86, 104663, (2023); https://doi.org/10.1016/j.jddst.2023.104663

[14]. J.S. Zhang, et al., Redox Biology, 37, 101715, (2020); https://doi.org/10.1016/j.redox.2020.101715

[15]. S.S. Martinez, et al., International Journal of Molecular Sciences, 23(1), 280, (2022); https://doi.org/10.3390/ijms23010280

[16]. A.R.A. Nassar, et al., Scientific Reports, 13(1), 9054, (2023); https://doi.org/10.1038/s41598-023-35360-9

[17]. S.J. Kim, et al., International Journal of Molecular Sciences, 22(21), 11844, (2021); https://doi.org/10.3390/ijms222111844

[18]. H.W. Zeng and G.F. Combs, Journal of Nutritional Biochemistry, 19(1), 1-7, (2008); https://doi.org/10.1016/j.jnutbio.2007.02.005

[19]. E.M. El-Fakharany, et al., Scientific Reports, 13(1), 9579, (2023); https://doi.org/10.1038/s41598-023-36492-8

[20]. J.A. Choi, et al., Journal of Clinical Oncology, 40(16), E17547-E17547, (2022); https://doi.org/10.1200/JCO.2022.40.16_suppl.e17547

[21]. X.L. Cai, et al., Scientific Reports, 6, 19213, (2016); https://doi.org/10.1038/srep19213

[22]. U. Tinggi, Environmental Heath and Preventive Medicine, 13, 102-108, (2008); https://doi.org/10.1007/s12199-007-0019-4

[23]. M.P. Rayman, Lancet, 356(9225), 233-241, (2000); https://doi.org/10.1016/S0140-6736(00)02490-9

[24]. Z. Huang, A.H. Rose, P.R. Hoffmann, Antioxidants & Redox Signaling, 16(7), 705-743, (2012); https://doi.org/10.1089/ars.2011.4145

[25]. P.A. Tran, et al., International Journal of Nanomedicine, 14, 4613-4624, (2019); https://doi.org/10.2147/IJN.S197737

[26]. K.K. Karthik, et al., Biomedical Technology, 6, 61-74, (2024); https://doi.org/10.1016/j.bmt.2023.12.001

[27]. N. Bisht, P. Phalswal, P.K. Khanna, Materials Advances, 3, 1415-1431, (2022); https://doi.org/10.1039/D1MA00639H

[28]. G. Guisbiers, Advances in Physics: X, 9, 2357809, (2024); https://doi.org/10.1080/23746149.2024.2357809

[29]. D.S. Zhang, B. Goekce, S. Barcikowski, Chemical Reviews, 117(5), 3990-4103, (2017); https://doi.org/10.1021/acs.chemrev.6b00468

[30]. E. Fazio, et al., Nanomaterials, 10(11), 2317, (2020); https://doi.org/10.3390/nano10112317

[31]. I.Y. Khairani, et al., Physical Chemistry Chemical Physics, 25, 19380-19408, (2023); https://doi.org/10.1039/D3CP01214J

[32]. M.-R. Kalus, et al., Materials Today Proceedings, 4, S93-S100, (2017); https://doi.org/10.1016/j.matpr.2017.09.173

[33]. P.A. Tran, T.J. Webster, International Journal of Nanomedicine, 6, 1553-1558, (2011); https://doi.org/10.2147/IJN.S21729

[34]. P.A. Tran, T.J. Webster, Nanotechnology, 24, 155101, (2013); https://doi.org/10.1088/0957-4484/24/15/155101

[35]. J.T. Seil, T.J. Webster, International Journal of Nanomedicine, 7, 2767-2781, (2012); https://doi.org/10.2147/ijn.s24805

[36]. W. Lu, et al., Journal of the American Chemical Society, 146, 6345-6351, (2024); https://doi.org/10.1021/jacs.4c00219

[37]. P. Cherin, P. Unger, Inorganic Chemistry, 6, 1589-1591, (1967); https://doi.org/10.1021/ic50054a037

[38]. R. Subedi, G. Guisbiers, ACS Omega, 9, 25832-25840, (2024); https://doi.org/10.1021/acsomega.3c10497

[39]. J. Stetefeld, S.A. McKenna, T.R. Patel, Biophysical Reviews, 8, 409-427, (2016); https://doi.org/10.1007/s12551-016-0218-6

[40]. G. Lucovsky, et al., Solid State Communications, 5, 113-117, (1967); https://doi.org/10.1016/0038-1098(67)90006-3

[41]. S.N. Yannopoulos, K.S. Andrikopoulos, Journal of Chemical Physics, 121(10), 4747-4758, (2004); https://doi.org/10.1063/1.1780151

[42]. M.A. Ruiz-Fresneda, et al., Microbial Biotechnology, 16, 877-892, (2023); https://doi.org/10.1111/1751-7915.14209

[43]. S. Bhattacharjee, Journal of Controlled Release, 235, 337-351, (2016); https://doi.org/10.1016/j.jconrel.2016.06.017

[44]. L.-H. Lee, Journal of Non-Crystalline Solids, 6, 213-220, (1971); https://doi.org/10.1016/0022-3093(71)90004-4

[45]. G. Guisbiers, S. Arscott, R. Snyders, Applied Physics Letters, 101, 231606, (2012); https://doi.org/10.1063/1.4769358

[46]. H.H. Tuson, D.B. Weibel, Soft Matter, 14, 4368-4380, (2013); https://doi.org/10.1039/c3sm27705d

[47]. L.D. Renner, D.B. Weibel, MRS Bulletin, 36, 347-355, (2011); https://doi.org/10.1557/mrs.2011.65

[48]. C.E. Hassan, T.J. Webster, International Journal of Nanomedicine, 11, 3641-3654, (2016); https://doi.org/10.2147/IJN.S105173

[49]. K. Li, et al., Journal of Hazardous Materials, 465, 133287, (2024); https://doi.org/10.1016/j.jhazmat.2023.133287